Technical University of Denmark

DTU

The equivalent static loads method for structural optimization does not in general generate optimal designs

Stolpe, Mathias; Verbart, Alexander; Rojas Labanda, Susana

DTU Library
Technical Information Center of Denmark

The Equivalent Static Loads Method for structural optimization does not in general generate optimal designs

Mathias Stolpe   Alexander Verbart   Susana Rojas Labanda [*]

October 18, 2017

Abstract

The Equivalent Static Loads Method (ESLM) is an algorithm intended for dynamic response structural optimization. The algorithm attempts to solve a sequence of static response structural optimization problems approximating the original problem. It is argued in several published articles that if the ESLM converges then it finds a KKT point of the considered dynamic structural response optimization problem. The theoretical convergence properties of the ESLM are however not as strong as previously reported. We propose and analyze easily reproducible counter examples based on a two-bar truss illustrating that the ESLM in general fails in finding optimal designs to the considered dynamic response problem.

Keywords: Structural optimization, Equivalent Static Loads Method, Convergence properties, Sensitivity analysis

1   Introduction

The Equivalent Static Loads Method (ESLM) has been proposed for various applications of dynamic response structural optimization over a number of years. Notable articles include [5], [8], [6], [12], and [14] among others. One of the main theoretical results regarding the Equivalent Static Loads Method for structural optimization with transient analysis is stated in [12]. The assertion is that when the ESLM converges then the primal dual KKT point[1] of the final static response sub-problem is also a primal dual KKT point of the original dynamic response problem. The proof provided in [12] was challenged in [15] as incomplete and partially incorrect. The correctness of the result itself has been left open until now. We illustrate that the assertion from [12] in general is not correct by proposing and solving several problem instances obtained from different problem formulations which contradict the result. Additionally, the examples illustrate that the ESLM does not in general converge to optimal designs. We also explain the fundamental reasons for the failure of the ESLM to solve these examples.

The problems in this article have been purposely designed with a number of specifications in mind. The objective and constraint functions in the dynamic response problem are

---

[*]DTU Wind Energy, Technical University of Denmark, Frederiksborgvej 399, 4000 Roskilde, Denmark. E-mail: `matst@dtu.dk,alev@dtu.dk,srla@dtu.dk`

[1]We use the term KKT point to refer to a feasible point $\mathbf{x}^*$ for which there exist positive Lagrange multipliers satisfying the KKT conditions to the studied inequality constrained problem. The term primal dual KKT point refers to the pair $(\mathbf{x}^*, \boldsymbol{\lambda}^*)$ satisfying the KKT conditions.
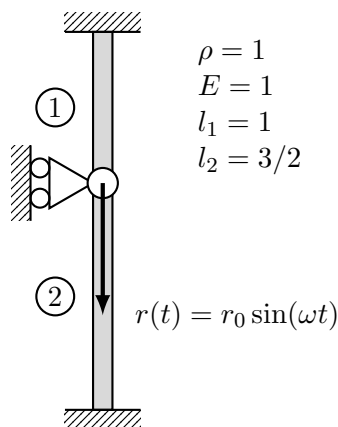
Figure 1: Ground structure for the two-bar truss examples including boundary conditions and external load.

chosen such that the static response sub-problems in the ESLM become well-defined convex optimization problems. The sub-problems are ensured to have non-empty feasible sets which additionally satisfy standard constraint qualifications. The structural model and problem size and data are chosen such that the static response sub-problems each have a unique optimal solution and can be solved analytically. The structural model is such that for each point satisfying the constraints the structural analysis also has a unique solution and that the design sensitivity analysis is well-defined. This implies that, for the proposed problems, all steps of the ESLM are well-defined.

The examples are based on standard concepts in terms of structural modeling and standard techniques for structural analysis and design sensitivity analysis. Additionally, the stiffness and mass matrices are explicitly given as functions of the design variables. The examples and the results from this article are thus easily reproducible.

1.1 Brief outline of the methodology and results

We present and study several variants of truss sizing optimization problems based on dynamic response analysis. The ground structure on which all results are based is shown in Figure 1 for some appropriately chosen material and problem data. The design variables x_1 and x_2 represent the cross-sectional areas of the two bars, respectively. The problems in this article thus have an almost minimal number of design variables (equal to two) and a minimal number of degrees of freedom for the structural analysis (equal to one). The objective function is chosen to be the dynamic compliance, in the sense that it becomes weighted static compliance in the static response sub-problem. The constraints include lower and upper bounds on the design variables and a limit on the total volume of the structure. The static response sub-problems are classical minimum compliance truss sizing problems with advantageous properties including convexity of the objective function and the feasible set, satisfaction of standard constraint qualifications, and existence and uniqueness of an optimal solution. The external load is sinusoidal with a driving frequency ω and a nominal amplitude $r_0 = 1$.

The contours of the objective function of one of the dynamic response problems and the feasible set are illustrated in Figure 2. The feasible set is illustrated by the light grey triangle. The manuscript confirms the following statements both by analytic and numerical

2

approaches. The minimum to the dynamic response problems is located at $\mathbf{x}^* = (1/10\ 6/10)^T$ and this is a KKT point since the directional derivatives of the objective are strictly positive in all directions in the tangent cone [11]. For this particular problem, a standard version of the ESLM converges, *independent of the starting point*, to the point $\hat{\mathbf{x}} = (17/20\ 1/10)^T$ in at most two iterations, i.e. static response sub-problems solved. The point $\hat{\mathbf{x}}$ is however not a local minimum, and therefore, not a KKT point to the considered dynamic response problems. Figure 2 illustrates that at $\hat{\mathbf{x}}$ there is a feasible descent direction (towards $\mathbf{x}^*$) such that the directional derivative of the objective is negative. Thus, it is possible to find a feasible point $\mathbf{x}$ in the neighborhood of $\hat{\mathbf{x}}$ such that $f(\mathbf{x}) < f(\hat{\mathbf{x}})$. These results are later described in more detail and verified both analytically and numerically.
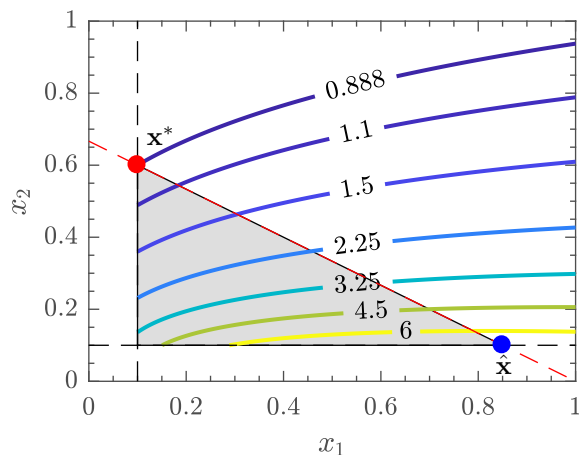
Figure 2: Design domain of the dynamic response problem. The contour lines represent the objective function values, and the dotted lines the constraint surfaces. The grey area enclosed by the dotted lines represents the feasible set.

Notation and units

The notation $\mathbf{A} \succeq \mathbf{B}$ ($\succ$) where $\mathbf{A}$ and $\mathbf{B}$ are square matrices of the same size means that $\mathbf{A} - \mathbf{B}$ is positive semi-definite (positive definite). The interior of a set X is denoted $\mathrm{int}(X)$. The sub-index i is used to denote a particular point in time whereas the super-index k is used for iterates of the ELSM. SI units are used through out the article.

2 General problem formulations, assumptions, and the ESLM

This section contains the general formulations of the considered problem in both continuous time and discrete time, and a standard statement of the ESLM algorithm for discrete time problems.

2.1 Dynamic response optimization problem

We consider the following dynamic response structural optimization problem in the design variables $\mathbf{x} \in \mathbb{R}^n$

$$\begin{aligned}
\underset{\mathbf{x} \in \mathbb{R}^n}{\text{minimize}} \quad & f(\mathbf{x}, \mathbf{u}(\mathbf{x}, t)) \\
\text{subject to} \quad & c_j(\mathbf{x}, \mathbf{u}(\mathbf{x}, t)) \leq 0 \quad j = 1, \ldots, m \\
& \mathbf{x} \in X,
\end{aligned} \qquad (\mathcal{G}_C)$$

where $X \subseteq \mathbb{R}^n$ is a, for now, unspecified set and m is the number of nonlinear constraint functions. The displacement vector $\mathbf{u}(\mathbf{x}, t)$ comes from dynamic response analysis in the time domain. Note that $(\mathcal{G}_C)$ in general is a semi-infinite optimization problem since the nonlinear constraints $c_j(\mathbf{x}, \mathbf{u}(\mathbf{x}, t)) \leq 0$ should be satisfied for all relevant t in some given time interval.

The structural analysis equations are assumed to be

$$\mathbf{M}(\mathbf{x})\ddot{\mathbf{u}}(\mathbf{x}, t) + \mathbf{C}(\mathbf{x})\dot{\mathbf{u}}(\mathbf{x}, t) + \mathbf{K}(\mathbf{x})\mathbf{u}(\mathbf{x}, t) = \mathbf{r}(t) \text{ for } t \in [0, T] \qquad (1)$$

with the initial conditions at rest, i.e. $\mathbf{u}(0) = \mathbf{0}$, and $\dot{\mathbf{u}}(0) = \mathbf{0}$. $\mathbf{M}(\mathbf{x})$, $\mathbf{C}(\mathbf{x})$, and $\mathbf{K}(\mathbf{x})$ denote the mass, damping, and stiffness matrices, respectively. The velocity and acceleration vectors are defined by $\dot{\mathbf{u}}(\mathbf{x}, t)$ and $\ddot{\mathbf{u}}(\mathbf{x}, t)$, respectively. To simplify the design sensitivity analysis it is assumed that both the initial conditions and the external load $\mathbf{r}(t)$ are design independent. The structural analysis equations obtained after discretizing the time interval $[0, T]$ into N equally long segments of time Δt are

$$\mathbf{M}(\mathbf{x})\ddot{\mathbf{u}}_i(\mathbf{x}) + \mathbf{C}(\mathbf{x})\dot{\mathbf{u}}_i(\mathbf{x}) + \mathbf{K}(\mathbf{x})\mathbf{u}_i(\mathbf{x}) = \mathbf{r}_i \text{ for } i = 0, 1, \ldots, N \qquad (2)$$

with the initial conditions at rest, i.e. $\mathbf{u}_0 = \mathbf{0}$, and $\dot{\mathbf{u}}_0 = \mathbf{0}$. Throughout the article we assume that the following conditions are satisfied.

(A1) The stiffness matrix is linear in the design variables $\mathbf{K}(\mathbf{x}) = \sum_{j=1}^n x_j \mathbf{K}_j$ and the mass matrix is linear in the design variables $\mathbf{M}(\mathbf{x}) = \sum_{j=1}^n x_j \mathbf{M}_j$ where $\mathbf{K}_j = \mathbf{K}_j^T \succeq \mathbf{0}$ and $\mathbf{M}_j = \mathbf{M}_j^T \succeq \mathbf{0}$ for $j = 1, \ldots, n$.

(A2) $\mathbf{M}(\mathbf{x}) \succ \mathbf{0}$, $\mathbf{C}(\mathbf{x}) \succ \mathbf{0}$, and $\mathbf{K}(\mathbf{x}) \succ \mathbf{0}$ for all $\mathbf{x} \in X$.

The linear dependence in (A1) on the design variables in both mass and stiffness matrices is standard for topology and sizing optimization problems of trusses, see e.g. [2]. Assumption (A2) is also common for sizing optimization problems and states that the structure is appropriately supported and all members have mass and stiffness if the design variables are strictly positive.

The time-discretized optimization problem approximating $(\mathcal{G}_C)$ is then formulated as

$$\begin{aligned}
\underset{\mathbf{x} \in \mathbb{R}^n}{\text{minimize}} \quad & f(\mathbf{x}, \mathbf{u}(\mathbf{x})) \\
\text{subject to} \quad & c_j(\mathbf{x}, \mathbf{u}(\mathbf{x})) \leq 0 \quad j = 1, \ldots, m, \\
& \mathbf{x} \in X.
\end{aligned} \qquad (\mathcal{G}_D)$$

Here, the $\mathbf{u}(\mathbf{x})$ contains all the displacement vectors at each time step, i.e.

$$\mathbf{u}(\mathbf{x}) = \begin{pmatrix} \mathbf{u}_0(\mathbf{x})^T & \cdots & \mathbf{u}_N(\mathbf{x})^T \end{pmatrix}^T.$$

4

Problem $(\mathcal{G}_D)$ is slightly different from the most common statements found in the literature on the ESLM in that the objective function is not only an explicit function of the design variables and that the constraints include all time steps rather than just one. This choice of formulation is intended to simplify the visual presentation of the examples and does not influence the results or conclusions. A modified version of the examples which satisfies the problem format from e.g. [12] is presented in Appendix A.

2.2 Equivalent static load method

Instead of solving Problem $(\mathcal{G}_D)$ directly, the equivalent static load method attempts to solve a sequence of static response sub-problems. The sub-problem at iteration k in the ESLM presented in Algorithm 1 corresponding to $(\mathcal{G}_D)$ becomes

$$
\begin{aligned}
\underset{\mathbf{x} \in \mathbb{R}^n}{\text{minimize}} \quad & f(\mathbf{x}, \mathbf{w}^{\mathbf{x}^k}(\mathbf{x})) \\
\text{subject to} \quad & c_j(\mathbf{x}, \mathbf{w}^{\mathbf{x}^k}(\mathbf{x})) \leq 0 \quad j = 1, \ldots, m \\
& \mathbf{x} \in X
\end{aligned}
\tag{$\mathcal{P}^k$}
$$

Here, $\mathbf{w}^{\mathbf{x}^k}(\mathbf{x}) = \left(\mathbf{w}_0(\mathbf{x})^T \quad \cdots \quad \mathbf{w}_N(\mathbf{x})^T \right)^T$ is such that $\mathbf{w}_i(\mathbf{x})$ is the solution to the static analysis problem

$$
\mathbf{K}(\mathbf{x})\mathbf{w}_i(\mathbf{x}) = \mathbf{r}_i^e(\mathbf{x}^k) \text{ for } i = 0, \ldots, N,
\tag{3}
$$

where $\mathbf{r}^e(\mathbf{x}^k)$ are the equivalent static loads evaluated at $\mathbf{x}^k$. The equivalent static loads are defined as

$$
\mathbf{r}_i^e(\mathbf{x}) = \mathbf{K}(\mathbf{x})\mathbf{u}_i(\mathbf{x}) \text{ for } i = 0, \ldots, N.
\tag{4}
$$

The equivalent static loads $\mathbf{r}_i^e$ are thus defined as those loads that produce the same displacements at all times as the dynamic response analysis, respectively. For simplicity, throughout the rest of the article, $\mathbf{w}^{\mathbf{x}^k}(\mathbf{x})$ is denoted by $\mathbf{w}(\mathbf{x})$.

Remark 1. *It should be noted that while solving the static response sub-problem ($\mathcal{P}^k$) the static loads are design independent since they are ESLs evaluated at the current (outer) iterate $\mathbf{x}^k$.*

An ESLM algorithm is restated for completeness in Algorithm 1 below. The algorithm is slightly different in notation compared to previous statements in e.g. [12] or [15] and it is also modified for the class of problem studied. The algorithm terminates when the equivalent static loads of two consecutive outer iterations are almost identical or alternatively when two consecutive iterates are close in some norm. The first stopping condition was suggested in e.g. [12]. The second stopping condition is stronger since it implies the first. In the following numerical experiments both stopping conditions are satisfied simultaneously.

The stated ESLM algorithm does not contain any measures to enforce convergence such as move limits, trust regions, or merit functions, etc. This is not required to ensure convergence for the examples presented below and it was not specified in [12] how such measure should be incorporated.

Remark 2. *The optimization problem presented in the ESLM is formulated in a time-discrete space. However, the ESLM static response sub-problem can also be defined in a continuous time.*

Algorithm 1: Equivalent static loads algorithm for the dynamic structural design problems $(\mathcal{G}_D)$.

Initialize $\mathbf{x}^0 \in X$. Initialize the convergence tolerances $\epsilon_f > 0$ and $\epsilon_x > 0$.

Set $k = 0$ and continue = `true`.

while *continue* **do**

  Perform the transient analysis in (2) with $\mathbf{x} = \mathbf{x}^k$.

  Compute the equivalent static loads

  $$\mathbf{r}_i^e(\mathbf{x}^k) = \mathbf{K}(\mathbf{x}^k)\mathbf{u}_i(\mathbf{x}^k) \text{ for } i = 0, 1, \ldots, N.$$

  if $k > 1$ *and* $(\|\mathbf{r}_i^e(\mathbf{x}^k) - \mathbf{r}_i^e(\mathbf{x}^{k-1})\| < \epsilon_f \; \forall \; i \; or \; \|\mathbf{x}^k - \mathbf{x}^{k-1}\| < \epsilon_x)$ **then**

    Set continue = `false`.

  else

    Attempt to solve the static response problem (5)

    $$\begin{aligned} \underset{\mathbf{x} \in \mathbb{R}^n}{\text{minimize}} \quad & f(\mathbf{x}, \mathbf{w}(\mathbf{x})) \\ \text{subject to} \quad & c_j(\mathbf{x}, \mathbf{w}(\mathbf{x})) \leq 0 \quad j = 1, \ldots, m \\ & \mathbf{x} \in X. \end{aligned} \quad (5)$$

    where $\mathbf{w}_i(\mathbf{x})$ is the unique solution to the static equilibrium equations

    $$\mathbf{K}(\mathbf{x})\mathbf{w}_i(\mathbf{x}) = \mathbf{r}_i^e(\mathbf{x}^k) \text{ for } i = 0, 1, \ldots, N. \quad (6)$$

    Denote the found design $\hat{\mathbf{x}}^k$ and the associated Lagrange multipliers $\hat{\boldsymbol{\lambda}}^k$.

    Update the primal iterate $\mathbf{x}^{k+1} = \hat{\mathbf{x}}^k$ and Lagrange multipliers $\boldsymbol{\lambda}^{k+1} = \hat{\boldsymbol{\lambda}}^k$.

    Update the iteration counter $k \leftarrow k + 1$.

  end

  Let $(\hat{\boldsymbol{x}}, \hat{\boldsymbol{\lambda}}) = (\mathbf{x}^k, \boldsymbol{\lambda}^k)$.

end

2.3 On the KKT conditions for problems $(\mathcal{G}_D)$ and $(\mathcal{P}^k)$

If the ESLM converges (in the sense outlined in Algorithm 1) to a primal dual KKT point $(\hat{\mathbf{x}}, \hat{\boldsymbol{\lambda}})$, with $\hat{\boldsymbol{\lambda}}$ the vector with corresponding Lagrange multipliers, the point is also a primal dual KKT point of the original dynamic response problem if and only if the KKT conditions for both problem formulations are satisfied. In particular, if $(\hat{\mathbf{x}}, \hat{\boldsymbol{\lambda}})$ is a KKT point to the final static response sub-problem then by the construction of the algorithm both (primal and dual) feasibility and complementarity conditions are satisfied for the dynamic response problem, see e.g. [15]. However, in order to have identical first-order necessary optimality conditions, the displacement sensitivities in both formulations must be identical [15], i.e.

$$\frac{\partial \mathbf{w}_i(\hat{\mathbf{x}})}{\partial x_j} = \frac{\partial \mathbf{u}_i(\hat{\mathbf{x}})}{\partial x_j} \text{ for } i = 0, \ldots, N, \text{ and } j = 1, \ldots n. \tag{7}$$

The displacement sensitivities are obtained from differentiating the different state equations for both problems. For the dynamic response problem, the design sensitivities of displacements with respect to the jth variable at time step i are given by $\boldsymbol{\eta}_{ij} = \frac{\partial \mathbf{u}_i}{\partial x_j}$ solving the system (see e.g. [4])

$$\mathbf{M}(\mathbf{x})\ddot{\boldsymbol{\eta}}_{ij} + \mathbf{C}(\mathbf{x})\dot{\boldsymbol{\eta}}_{ij} + \mathbf{K}(\mathbf{x})\boldsymbol{\eta}_{ij} = -\left(\frac{\mathbf{M}(\mathbf{x})}{\partial x_j}\ddot{\mathbf{u}}_i + \frac{\mathbf{C}(\mathbf{x})}{\partial x_j}\dot{\mathbf{u}}_i + \frac{\mathbf{K}(\mathbf{x})}{\partial x_j}\mathbf{u}_i \right) \tag{8}$$

with the initial conditions at rest, i.e. $\boldsymbol{\eta}_{0j} = \mathbf{0}$, and $\dot{\boldsymbol{\eta}}_{0j} = \mathbf{0}$. The displacement sensitivities with respect to the jth variable at time step i of the static response sub-problem are

$$\frac{\partial \mathbf{w}_i(\mathbf{x})}{\partial x_j} = -\mathbf{K}^{-1}(\mathbf{x}) \frac{\partial \mathbf{K}(\mathbf{x})}{\partial x_j} \mathbf{w}_i(\mathbf{x}).$$

Since, $\mathbf{w}_i(\hat{\mathbf{x}}) = \mathbf{u}_i(\hat{\mathbf{x}}) \; \forall i$ by assumption (A2) and definition of equivalent static loads (4), both equations are equivalent only if the following conditions are satisfied at $\hat{\mathbf{x}}$

$$\frac{\partial \mathbf{M}(\hat{\mathbf{x}})}{\partial x_j} \ddot{\mathbf{u}}_i + \mathbf{M}(\hat{\mathbf{x}})\ddot{\boldsymbol{\eta}}_{ij} + \frac{\partial \mathbf{C}(\hat{\mathbf{x}})}{\partial x_j} \dot{\mathbf{u}}_i + \mathbf{C}(\hat{\mathbf{x}})\dot{\boldsymbol{\eta}}_{ij} = \mathbf{0} \text{ for } i = 0, \ldots, N, \text{ and } j = 1, \ldots n.$$

In Section 5, we demonstrate that this condition is not generally satisfied at a point of convergence of the ESLM.

3 The ESLM for a class of minimum compliance problems

This section presents a minimum compliance problem and the corresponding static response sub-problem.

3.1 Dynamic response optimization problem

The problem considered in this article is a special case of the following structural optimization problem

$$\underset{\mathbf{x} \in \mathbb{R}^n}{\text{minimize}} \quad f_c(\mathbf{x}) = \int_{t_1}^{t_2} \mathbf{u}(\mathbf{x}, t)^T \mathbf{K}(\mathbf{x})\mathbf{u}(\mathbf{x}, t) dt \tag{$\mathcal{P}_C$}$$

$$\text{subject to} \quad \mathbf{x} \in X$$

where $0 \leq t_1 < t_2 \leq T$. Since most literature on the ESLM covers the situation that the structural analysis is done numerically we also propose a time-discretized version of $(\mathcal{P}_C)$. One possible approximation of $(\mathcal{P}_C)$ based on a left Riemann sum becomes

$$\underset{\mathbf{x} \in \mathbb{R}^n}{\text{minimize}} \quad f(\mathbf{x}) = \sum_{i=\ell_1}^{\ell_2} f_i(\mathbf{x}) = \Delta t \sum_{i=\ell_1}^{\ell_2} \mathbf{u}_i(\mathbf{x})^T \mathbf{K}(\mathbf{x}) \mathbf{u}_i(\mathbf{x}) \qquad (\mathcal{P}_D)$$

$$\text{subject to} \quad \mathbf{x} \in X$$

where ℓ_1 and ℓ_2 are indices of the appropriately chosen time-points corresponding to t_1 and t_2, respectively. The set X is defined by linear inequality constraints

$$X = \{\mathbf{x} \in \mathbb{R}^n \mid \underline{\mathbf{x}} \leq \mathbf{x} \leq \overline{\mathbf{x}}, v(\mathbf{x}) = \sum_{j=1}^{n} x_j l_j - V \leq 0\},$$

where $\underline{\mathbf{x}}$ and $\overline{\mathbf{x}}$ are given lower and upper bounds on the design variables and $V > 0$ is a volume limit. Both $(\mathcal{P}_C)$ and $(\mathcal{P}_D)$ are special cases of problem $(\mathcal{G}_C)$ and $(\mathcal{G}_D)$ respectively, without any nonlinear constraint that depend on the displacements. Together with (A1) and (A2), we additionally assume that the following conditions are satisfied.

(A3) The variable bounds satisfy $0 < \underline{x}_j < \overline{x}_j < +\infty$ and the truss member length constants $l_j > 0$ for $j = 1, \ldots, n$.

(A4) The volume bound V satisfies $\sum_{j=1}^{n} \underline{x}_j l_j < V < \sum_{j=1}^{n} \overline{x}_j l_j$.

(A5) The damping is modelled by $\mathbf{C}(\mathbf{x}) = \mathbf{C}_0 + \alpha_K \mathbf{K}(\mathbf{x}) + \alpha_M \mathbf{M}(\mathbf{x})$ with $\mathbf{C}_0 \succeq \mathbf{0}$ as a given matrix and $\alpha_K \geq 0$ and $\alpha_M \geq 0$ as given constants.

Assumptions (A3) and (A4) ensure that the feasible set X is non-empty. Similar assumptions are also found in e.g. [1]. Assumption (A5) allows for different damping models including Rayleigh damping [7].

Remark 3. *In the examples only the steady-state part of the displacements are considered in the objective function in $(\mathcal{P}_C)$ whereas transient analysis is used for $(\mathcal{P}_D)$. In the examples the starting time for the integration t_1 is chosen sufficiently large and the system damping is high enough such that any initial transients have been damped out and can be neglected. We therefore choose to use the same notation for the displacements.*

3.2 The ESLM static response sub-problems

The static response sub-problems at iteration k in the ESLM presented in Algorithm 1 corresponding to the minimum compliance problems $(\mathcal{P}_C)$ and $(\mathcal{P}_D)$ become, respectively,

$$\underset{\mathbf{x} \in \mathbb{R}^n}{\text{minimize}} \quad \tilde{f}_{c,\mathbf{x}^k}(\mathbf{x}) = \int_{t_1}^{t_2} (\mathbf{r}^e(\mathbf{x}^k, t))^T \mathbf{K}^{-1}(\mathbf{x}) \mathbf{r}^e(\mathbf{x}^k, t) \qquad (\mathcal{S}_C)$$

$$\text{subject to} \quad \mathbf{x} \in X$$

with the equivalent static loads computed by

$$\mathbf{r}^e(\mathbf{x}^k, t) = \mathbf{K}(\mathbf{x}^k) \mathbf{u}(\mathbf{x}^k, t),$$

8

and

$$\underset{\mathbf{x}\in\mathbb{R}^n}{\text{minimize}} \quad \tilde{f}_{\mathbf{x}^k}(\mathbf{x}) = \Delta t \sum_{i=\ell_1}^{\ell_2} (\mathbf{r}_i^e(\mathbf{x}^k))^T \mathbf{K}^{-1}(\mathbf{x}) \mathbf{r}_i^e(\mathbf{x}^k) \tag{$\mathcal{S}_D$}$$
$$\text{subject to} \quad \mathbf{x} \in X.$$

The feasible set of the static response sub-problems $(\mathcal{S}_C)$ and $(\mathcal{S}_D)$ is non-empty under assumptions (A3)-(A4). Furthermore, since the constraints are linear they satisfy standard constraint qualifications [11]. The feasible set is also convex since it is a polyhedron [10]. Additionally the objective functions are both convex since the stiffness matrix is linear in the design variables [16] following assumption (A1). Since objective functions are continuously differentiable on the feasible set following assumptions (A1) and (A2) and the feasible set is compact (i.e. closed and bounded), existence of optimal solutions is ensured by Weierstrass theorem, see e.g. [9]. This implies that finding a KKT point is both necessary and sufficient for a global minimizer.

One important quality that cannot be ensured for the sub-problems is uniqueness of the optimal solution. However, for the small-scale example presented below there is only one optimal solution.

Remark 4. *With the stated assumptions (A1)-(A5) and the choice of problem formulations $(\mathcal{P}_C)$ and $(\mathcal{P}_D)$ every step of the ESLM in Algorithm 1 is well-defined. The analysis problems have unique solutions, the design sensitivities of the displacements are at least continuously differentiable ([4]), and the static response sub-problems can be numerically solved to proven global optimality due to convexity and the regularity properties.*

4   A two-bar truss example

For the remainder of this manuscript, we consider the two-bar structure shown in Figure 1. The structure consists of two-bars with different lengths. The top and bottom nodes are fixed whereas the middle node has a roller support. Consequently, the analysis contains only a single free degree of freedom. This is represented in the notation. The stiffness, mass, and damping "matrices" are from now on denoted $k(\mathbf{x})$, $m(\mathbf{x})$ and $c(\mathbf{x})$, respectively.

The structure is subjected to a harmonic load applied to the middle node. The load is defined as $r(t) = r_0 \sin(\omega t)$, where $r_0 = 1$ denotes the load amplitude, and $\omega = \pi/2$ its driving frequency. The material is assumed to be the same in the two-bars with Young's modulus $E_1 = E_2 = E = 1$ and density $\rho_1 = \rho_2 = \rho = 1$. The lengths of the bars are $l_1 = 1$ and $l_2 = 3/2$. The bounds on the design variables are set to $\underline{x}_1 = \underline{x}_2 = 1/10$ and $\overline{x}_1 = \overline{x}_2 = 1$. The volume limit is set to $V = 1$. The volume of the structure is defined as $x_1 l_1 + x_2 l_2 = x_1 + \frac{3}{2} x_2$. The damping is modelled by a damping coefficient c_0, which is chosen constant as $c_0 = 0.1$. The other damping parameters $\alpha_K = \alpha_M = 0$ and thus $c(\mathbf{x}) = c_0$. With these choices of structural model and problem data all the listed assumptions (A1)-(A5) are satisfied.

Optimization applied to the two-bar truss is based on its steady-state solution, i.e. neglecting its initial transient behaviour. The time domain we consider in the objective function is $t \in [t_1, t_1 + \frac{1}{2}T_\omega]$, where, $T_\omega = 2\pi/\omega$ is one time period of the driving frequency and t_1 is large enough for the initial transient behaviour to damp out in the numerical solution.

4.1 Analytical solution of the dynamic response problem

The two-bar truss can be represented by a forced, damped single-degree-of-freedom spring mass system (see Figure 1), which equation of motion is defined as

$$\ddot{u}(\mathbf{x}, t) + 2\zeta(\mathbf{x})\omega_n(\mathbf{x})\dot{u}(\mathbf{x}, t) + \omega_n^2(\mathbf{x})u(\mathbf{x}, t) = \frac{1}{m(\mathbf{x})}r_0\sin(\omega t) \quad \text{for } t \in [t_1, t_1 + \frac{1}{2}T_\omega]. \quad (9)$$

Here, $\omega_n(\mathbf{x}) = \sqrt{k(\mathbf{x})/m(\mathbf{x})}$ denotes the natural frequency, and $k(\mathbf{x})$ and $m(\mathbf{x})$ denote the representative spring stiffness and point mass, respectively. $\zeta(\mathbf{x}) = c(\mathbf{x})/\sqrt{4k(\mathbf{x})m(\mathbf{x})}$ is the damping ratio.

The representative point mass and spring stiffness are derived using truss finite elements, where a lumped mass approach is used for the mass matrix. After constructing the global matrices and removing the fixed degrees of freedom, the representative stiffness and point mass become

$$k(\mathbf{x}) = \frac{x_1 E_1}{l_1} + \frac{x_2 E_2}{l_2} = x_1 + \frac{2}{3}x_2$$

and

$$m(\mathbf{x}) = \frac{1}{2}x_1\rho_1 l_1 + \frac{1}{2}x_2\rho_2 l_2 = \frac{1}{2}x_1 + \frac{3}{4}x_2,$$

respectively.

The steady-state solution to (9) is

$$u(\mathbf{x}, t) = u_0(\mathbf{x})\sin(\omega t + \phi(\mathbf{x})),$$

where $u_0(\mathbf{x})$ and $\phi(\mathbf{x})$ denote the amplitude and phase shift defined as

$$u_0(\mathbf{x}) = \frac{r_0}{k(\mathbf{x})}\left[\left(1 - \frac{\omega^2}{\omega_n^2(\mathbf{x})}\right)^2 + \left(\frac{2\zeta(\mathbf{x})\omega}{\omega_n(\mathbf{x})}\right)^2\right]^{-\frac{1}{2}},$$

and

$$\phi(\mathbf{x}) = \arctan\left(\beta(\mathbf{x})\right) \quad \text{where } \beta(\mathbf{x}) = \frac{-2\zeta(\mathbf{x})\omega/\omega_n(\mathbf{x})}{1 - \omega^2/\omega_n^2(\mathbf{x})},$$

respectively (see e.g. [7]).

4.2 Dynamic compliance optimization problem

The dynamic compliance for the considered time domain is

$$f_c(\mathbf{x}) = k(\mathbf{x})u_0^2(\mathbf{x})\int\limits_{t_1}^{t_1 + \frac{\pi}{\omega}}\sin^2(\omega t + \phi(\mathbf{x}))\,\mathrm{d}t = \frac{\pi}{2\omega}k(\mathbf{x})u_0^2(\mathbf{x}), \quad (10)$$

which is independent of the phase shift for the chosen time domain of half the time period of the driving frequency $(T_\omega/2 = \pi/\omega)$.

Thus, the dynamic optimization response problem is defined for both the continuous and the discrete time domain as

$$\begin{aligned}\underset{\mathbf{x}\in\mathbb{R}^2}{\text{minimize}} \quad & f_c(\mathbf{x}) = (x_1 + \frac{2}{3}x_2)\frac{\pi}{2\omega}u_0(\mathbf{x})^2 \\ \text{subject to} \quad & \mathbf{x} \in X\end{aligned} \qquad (\mathrm{P_C^{II}})$$

10

and

$$\underset{\mathbf{x}\in\mathbb{R}^2}{\text{minimize}} \quad f(\mathbf{x}) = (x_1 + \frac{2}{3}x_2)\Delta t \sum_{i=l_1}^{l_2} u_i(\mathbf{x})^2 \tag{P_D^{II}}$$
$$\text{subject to} \quad \mathbf{x} \in X,$$

respectively.

4.3 Optimal solution to static response sub-problem

The objective function for the static response sub-problem for the equivalent static load method applied to (P_C^{II}) at iterate $\mathbf{x}^k$ becomes

$$\tilde{f}_{c,\mathbf{x}^k}(\mathbf{x}) = \frac{1}{k(\mathbf{x})} \int_{t_1}^{t_1+\frac{\pi}{\omega}} r^e(\mathbf{x}^k,t)^2 \, \mathrm{d}t = \frac{1}{k(\mathbf{x})} \frac{\pi}{2\omega} \left(k(\mathbf{x}^k)u_0(\mathbf{x}^k) \right)^2. \tag{11}$$

Note that the iterate point $\mathbf{x}^k$ does not change during the optimization of the sub-problem. Here, $r^e(\mathbf{x}^k, t)$ are the equivalent static loads for the dynamic response optimization problem, i.e.

$$r^e(\mathbf{x}, t) = k(\mathbf{x})u(\mathbf{x}, t). \tag{12}$$

evaluated at the outer iterate $\mathbf{x}^k$ for each sub-problem k in the ESLM. The displacements in the sub-problem at $\mathbf{x}^k$ are the solution to

$$w(\mathbf{x}, t) = \frac{1}{k(\mathbf{x})} r^e(\mathbf{x}^k, t). \tag{13}$$

The kth static response sub-problem for the two-bar truss problem in both the continuous (S_C^{II}) and the discrete (S_D^{II}) time domain become

$$\underset{\mathbf{x}\in\mathbb{R}^2}{\text{minimize}} \quad \tilde{f}_{c,\mathbf{x}^k}(\mathbf{x}) = \frac{1}{x_1 + \frac{2}{3}x_2} \frac{\pi}{2\omega} \left(k(\mathbf{x}^k)u_0(\mathbf{x}^k) \right)^2 \tag{S_C^{II}}$$
$$\text{subject to} \quad \mathbf{x} \in X$$

and

$$\underset{\mathbf{x}\in\mathbb{R}^2}{\text{minimize}} \quad \tilde{f}_{\mathbf{x}^k}(\mathbf{x}) = \frac{1}{x_1 + \frac{2}{3}x_2} \Delta t \sum_{i=l_1}^{l_2} \left(k(\mathbf{x}^k)u_i(\mathbf{x}^k) \right)^2 \tag{S_D^{II}}$$
$$\text{subject to} \quad \mathbf{x} \in X.$$

Minimizing the dynamic compliance (in both problem formulations (S_C^{II}) and (S_D^{II})) thus amounts to maximizing $x_1 + 2x_2/3$ for $\mathbf{x} \in X$ which is a linear optimization problem with a unique solution under the assumptions on the set X. The optimal design to the sub-problem is constructed by placing as much material in the shorter bar (while satisfying the volume constraint) and as little as possible in the longer bar while satisfying the lower bound constraints, i.e.

$$\hat{\mathbf{x}} = \begin{pmatrix} V - 3\underline{x}_2/2 \\ \underline{x}_2 \end{pmatrix} = \begin{pmatrix} 1 - 3/20 \\ 1/10 \end{pmatrix} = \frac{1}{20} \begin{pmatrix} 17 \\ 2 \end{pmatrix} = \begin{pmatrix} 0.85 \\ 0.10 \end{pmatrix}. \tag{14}$$

11

Remark 5. *The above discussion about the two-bar truss example has some very useful consequences. First of all, the optimal solution to the static response sub-problem is* independent *of the equivalent static loads* if at least one of them is non-zero. *The optimal objective function value still depends on the equivalent static loads. The situation that all equivalent static loads are zero is unlikely for this example. The sub-problem can also be solved analytically and the solution to the problems (S_C^{II}) and (S_D^{II}) for the two-bar truss example is* unique. *This shows that the ESLM outlined in Algorithm 1 performs, independent of the starting point, at most two iterations (i.e. static sub-problems solved) when applied to the two-bar truss examples.*

4.4   Graphical solution of the dynamic response problems

Figure 2 shows a graphical representation of the objective function of the original dynamic response problem (P_C^{II}) obtained by sampling the analytical expressions in 1000×1000 points in the domain $[0.1, 1] \times [0.1, 1]$. The plot shows the contour lines of the dynamic compliance objective, and the light grey region represents the feasible set, which is the area enclosed by the lower bounds on the design variables and the volume constraint. The blue point denotes the optimal design point $\hat{\mathbf{x}}$ obtained from application of the ESLM to the two-bar truss problem.

Figure 2 suggests that: *(i)* $\hat{\mathbf{x}}$ is not a (local) optimum to the dynamic response optimization problem, and *(ii)* the point

$$\mathbf{x}^* = \frac{1}{10} \begin{pmatrix} 1 \\ 6 \end{pmatrix} \tag{15}$$

is an optimal solution to the dynamic response problem (P_C^{II}).

5   Numerical validations

The two-bar truss example presented in Section 4 is used as a counter example to reveal that the Equivalent Static Load Method does not in general generate KKT points, and therefore, optimal designs. First of all, we numerically show that, as we anticipated, the ESLM converges to $\hat{\mathbf{x}}$ in at most two iterations, independent of the starting point. While this point is a KKT point (and local minimum) of the final static response problem, it is not a KKT point, and therefore, not a local minimum of the dynamic response problem. All the results reported in this section are validated analytically and numerically.

5.1   Implementation for numerical validation

The ESLM and the relevant analysis and sensitivity analysis routines have been implemented in Matlab 2016a specifically for the two-bar example independently by the three authors. Several different structural analysis techniques (i.e. time-discretization schemes) and corresponding design sensitivity analysis techniques are used. The implemented approaches lead to exactly the same overall behaviour and results. The Sequential Quadratic Programming (SQP) method implemented in `fmincon` is used to numerically solve all optimization problems.

   In the first implementation the Newmark average acceleration method (see e.g. [7]) is used for solving the governing dynamic response equations (2) and the system (8) to compute

12

design sensitivities. The second version uses the Runge-Kutta algorithm implemented in the function `ode45` (see e.g. [13]) for solving the governing equations (2) and the system (8). Here, the governing equations are reformulated as a system of first-order differential equations. The Runge-Kutta solver was instructed to output the state variables at equidistant time-points. The solvers do however call the user-supplied routines at other time steps and the displacement, velocities, and accelerations are therefore interpolated using the piecewise cubic hermite polynomials as implemented in the function `pchip` for use when solving the system (8).

The tolerances used for the convergence tests in Algorithm 1 are $\epsilon_x = \epsilon_f = 10^{-10}$. For the optimization solver default values on parameters and tolerances are used. For the numerical time integration we use a time step size of $\Delta t = 0.02$, and the objective function value is considered in the time domain $t \in [t_1, t_1 + \frac{\pi}{\omega}]$, where $t_1 = 200$.

5.2 Convergence of the ESLM for the two-bar truss example

We apply the ESLM from Algorithm 1 on the two-bar truss problems $(\mathrm{P_C^{II}})$ and $(\mathrm{P_D^{II}})$ and with the static response sub-problems modeled as convex problems. This produces a sequence of designs $\{\mathbf{x}^k\}$ and corresponding Lagrange multipliers. All implementations validate the theoretically anticipated behaviour of the algorithm. The ESLM in Algorithm 1 performs, independent of the starting point, at most two iterations (i.e. static sub-problems solved) when applied to the two-bar truss examples. The sequence of designs generated by the ESLM converges to the point $\hat{\mathbf{x}}$. The Algorithm stops due to the convergence criteria in the ESLM, i.e. given some tolerance $\epsilon_x > 0$ we obtain $\|\mathbf{x}^k - \mathbf{x}^{k-1}\| \le \epsilon_x$ and $\|\mathbf{r}_i^e(\mathbf{x}^k) - \mathbf{r}_i^e(\mathbf{x}^{k-1})\| \le \epsilon_f$ $\forall i$ and for $k = 1$ or $k = 2$ depending on the starting point.

Figure 3 shows the design domain for each of the two consecutive ESLM static response sub-problems starting from the minimum to the original dynamic response problem, $\mathbf{x}^0 = \mathbf{x}^*$. The first sub-problem converges to $\hat{\mathbf{x}}^0$, which is then the initial point to the second sub-problem $\mathbf{x}^1$. In the second sub-problem, the equivalent static loads are then evaluated in the point $\mathbf{x}^1$. The second sub-problem convergences $\hat{\mathbf{x}}^1 = \hat{\mathbf{x}}$ after which the algorithm terminates.

It is confirmed numerically that if the starting point is chosen as $\hat{\mathbf{x}}$ then only one iteration is performed before the algorithm terminates, otherwise two iterations are performed. This has a very severe implication. *If the ESLM is started at the KKT point (and global minimizer) for the dynamic response problem then the ESLM moves to a feasible point with inferior objective function value.*

5.2.1 The point $\hat{\mathbf{x}}$ is a KKT point (and a local minimum) of the static response problems $(\mathrm{S_C^{II}})$ and $(\mathrm{S_D^{II}})$

The point $\hat{\mathbf{x}}$ is a local solution of the static sub-problem of the ESLM if for all directions $\mathbf{d}$ in the tangent cone,

$$\nabla \tilde{f}_{c,\hat{\mathbf{x}}}(\hat{\mathbf{x}})^T \mathbf{d} > 0.$$

For the feasible set X, the tangent cone at $\hat{\mathbf{x}}$ is the convex combination of the two feasible direction $\hat{\mathbf{d}}_1$ and $\hat{\mathbf{d}}_2$, where

$$\hat{\mathbf{d}}_1 = \mathbf{x}^* - \hat{\mathbf{x}} = \frac{1}{4}\begin{pmatrix} -3 \\ 2 \end{pmatrix} \text{ and } \hat{\mathbf{d}}_2 = \begin{pmatrix} -1 \\ 0 \end{pmatrix}.$$
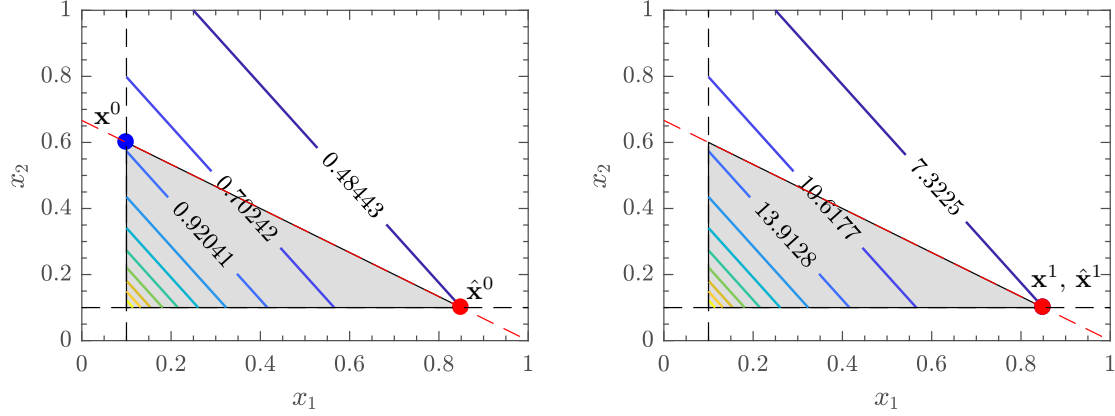
13

Figure 3: Objective functions for two consecutive static response sub-problems. Here, $\mathbf{x}^0$ denotes the initial design point, and $\hat{\mathbf{x}}^k$ denotes the point of convergence in the kth sub-problem. The equivalent static loads for the sub-problems are evaluated at $\mathbf{x}^k$. In the first sub-problem, $\mathbf{x}^k$ corresponds with the minimum of the dynamic response problem $\mathbf{x}^*$ (left), and the second sub-problem in which $\mathbf{x}^k$ coincides with the point $\hat{\mathbf{x}}$ that the ESLM converges to (right).

Table 1 lists the derivatives of the objective function of the static response sub-problem $(\mathrm{S}_{\mathrm{C}}^{\mathrm{II}})$ evaluated at $\hat{\mathbf{x}}$. For more details of the analytical expressions of the sensitivities see Appendix B.

Table 1: Value of the objective function of the static response sub-problem $(\mathrm{S}_{\mathrm{C}}^{\mathrm{II}})$ and its sensitivities evaluated at $\hat{\mathbf{x}}$ obtained from the analytical solution.

$\tilde{f}_{c,\hat{\mathbf{x}}}(\hat{\mathbf{x}})$	$\dfrac{\partial \tilde{f}_{c,\hat{\mathbf{x}}}(\hat{\mathbf{x}})}{\partial x_1}$	$\dfrac{\partial \tilde{f}_{c,\hat{\mathbf{x}}}(\hat{\mathbf{x}})}{\partial x_2}$
7.32253	-7.98821	-5.32547

It is confirmed that this point is a local minimum point to $(\mathrm{S}_{\mathrm{C}}^{\mathrm{II}})$ since the directional derivatives of the objective function are positive, i.e.

$$\nabla \tilde{f}_{c,\hat{\mathbf{x}}}(\hat{\mathbf{x}})^T \hat{\mathbf{d}}_1 = 3.32842$$
$$\nabla \tilde{f}_{c,\hat{\mathbf{x}}}(\hat{\mathbf{x}})^T \hat{\mathbf{d}}_2 = 7.98821.$$

Thus, it is a KKT point to $(\mathrm{S}_{\mathrm{C}}^{\mathrm{II}})$.

Additionally, we can show that the primal dual point $(\hat{\mathbf{x}}, \hat{\boldsymbol{\lambda}})$ satisfy the first-order optimality conditions for the static response problem $(\mathrm{S}_{\mathrm{C}}^{\mathrm{II}})$. The KKT conditions of problem $(\mathrm{S}_{\mathrm{C}}^{\mathrm{II}})$ at the point $(\hat{\mathbf{x}}, \hat{\boldsymbol{\lambda}})$, with $\hat{\boldsymbol{\lambda}} = (\hat{\lambda}, \hat{\boldsymbol{\xi}}, \hat{\boldsymbol{\mu}})$ are defined in (16). Here, $\hat{\lambda}$ represents the Lagrange multiplier of the volume constraint, and $\hat{\boldsymbol{\xi}}$, $\hat{\boldsymbol{\mu}}$ the Lagrange multipliers of the lower and upper

14

bounds at $\hat{\mathbf{x}}$, respectively.

$$\nabla \mathcal{L}(\hat{\mathbf{x}}, \hat{\boldsymbol{\lambda}}) = \nabla \tilde{f}_{c,\hat{\mathbf{x}}}(\hat{\mathbf{x}}) + \hat{\lambda} \nabla v(\hat{\mathbf{x}}) - \hat{\boldsymbol{\xi}} + \hat{\boldsymbol{\mu}} = \mathbf{0}, \tag{16a}$$

$$v(\hat{\mathbf{x}}) \leq 0, \quad \hat{\lambda} \geq 0, \tag{16b}$$

$$\underline{\mathbf{x}} - \hat{\mathbf{x}} \leq \mathbf{0}, \quad \hat{\boldsymbol{\xi}} \geq \mathbf{0}, \tag{16c}$$

$$\hat{\mathbf{x}} - \overline{\mathbf{x}} \leq \mathbf{0}, \quad \hat{\boldsymbol{\mu}} \geq \mathbf{0}, \tag{16d}$$

$$v(\hat{\mathbf{x}}) \hat{\lambda} = 0, \tag{16e}$$

$$(\underline{x} - \hat{x}_i) \hat{\xi}_i = 0, \quad i = 1, 2, \tag{16f}$$

$$(\hat{x}_i - \overline{x}_i) \hat{\mu}_i = 0, \quad i = 1, 2. \tag{16g}$$

At the point $\hat{\mathbf{x}}$, the Linear Independence Constraint Qualification (LICQ) are satisfied. This ensures that the Lagrange multipliers are unique [11]. From the optimality condition (16a), the Lagrange multipliers for the active volume constraint and lower bound of x_2 are explicitly defined in terms of the sensitivities:

$$
\begin{aligned}
\hat{\lambda} &= -\frac{\partial \tilde{f}_{c,\hat{\mathbf{x}}}(\hat{\mathbf{x}})}{\partial x_1} \left(\frac{\partial v(\hat{\mathbf{x}})}{\partial x_1} \right)^{-1} = -\frac{\partial \tilde{f}_{c,\hat{\mathbf{x}}}(\hat{\mathbf{x}})}{\partial x_1} = 7.98821 \\
\hat{\xi}_2 &= \frac{\partial \tilde{f}_{c,\hat{\mathbf{x}}}(\hat{\mathbf{x}})}{\partial x_2} + \hat{\lambda} \frac{\partial v(\hat{\mathbf{x}})}{\partial x_2} = \frac{\partial \tilde{f}_{c,\hat{\mathbf{x}}}(\hat{\mathbf{x}})}{\partial x_2} + \hat{\lambda} \frac{3}{2} = 6.65685
\end{aligned}
\tag{17}
$$

The other constraints are inactive at $\hat{\mathbf{x}}$, and therefore, $\hat{\xi}_1 = \hat{\mu}_1 = \hat{\mu}_2 = 0$ (16e-16g). Since all the KKT conditions are satisfied, the point $(\hat{\mathbf{x}}, \hat{\boldsymbol{\lambda}})$ is a KKT point.

These results are validated with the numerical implementations. The ESLM is solved using the SQP implemented in `fmincon` with two different time integration approaches. The partial derivatives of the dynamic compliance of the static sub-problem for both approaches are gathered in Table 2. Additionally, Table 2 shows the values of $\hat{\lambda}$ and $\hat{\xi}_2$ obtained from these simulations. These results are the same independent of the starting point.

Table 2: Value of the objective function of the ESLM static response sub-problem, its sensitivities evaluated at $\hat{\mathbf{x}}$, and the Lagrange multiplier values of the active constraints. The ESLM static response sub-problem is solved with an SQP method. Two different numerical integration schemes are used for the structural analysis and design sensitivity analysis.

Method	$\tilde{f}_{\hat{\mathbf{x}}}(\hat{\mathbf{x}})$	$\dfrac{\partial \tilde{f}_{\hat{\mathbf{x}}}(\hat{\mathbf{x}})}{\partial x_1}$	$\dfrac{\partial \tilde{f}_{\hat{\mathbf{x}}}(\hat{\mathbf{x}})}{\partial x_2}$	$\hat{\lambda}$	$\hat{\xi}_2$
SQP+Newmark's	7.31477	-7.97974	-5.31983	7.97974	6.64979
SQP+Runge Kutta	7.32253	-7.98821	-5.32547	7.98821	6.65684

5.3 The point $(\hat{\mathbf{x}}, \hat{\boldsymbol{\lambda}})$ is not a primal dual KKT point of the dynamic response problems (P_C^{II}) and (P_D^{II})

The main question is whether the primal dual point $(\hat{\mathbf{x}}, \hat{\boldsymbol{\lambda}})$ is a KKT point to the dynamic response problems (P_C^{II}) and (P_D^{II}). This is the claim from [12]. There are several ways to justify a negative answer to this question.
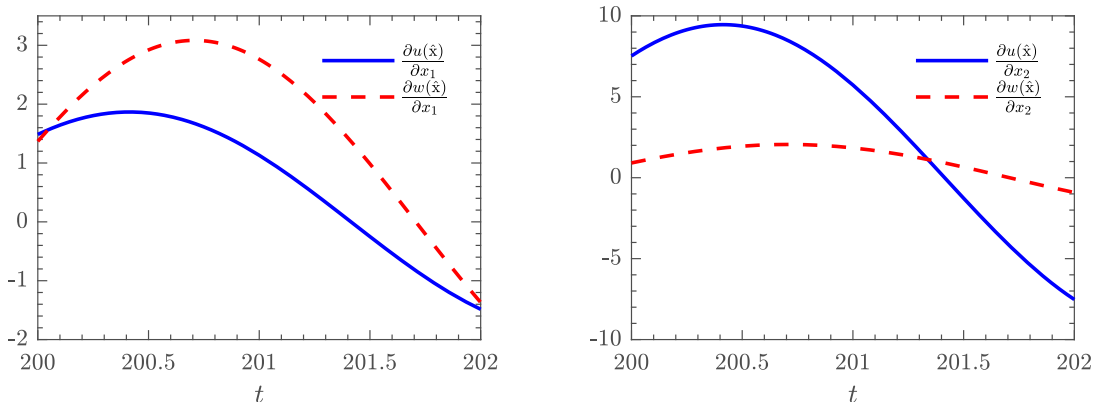
Figure 4: Displacement sensitivities at the point $\hat{\mathbf{x}}$ for both problem formulations (P_C^{II}) and (S_C^{II}). Displacement sensitivities with respect to x_1 (left), and displacement sensitivities with respect to x_2 (right). The displacement sensitivities are not identical, and therefore, the KKT conditions are not identical for both problem formulations.

5.3.1 Approach 1: The displacement sensitivities at $\hat{x}$ are different

In order for the KKT conditions for both formulations to be satisfied at $(\hat{\mathbf{x}}, \hat{\boldsymbol{\lambda}})$, it is a necessary condition that the displacement sensitivities for both formulations are identical; i.e. (7) should hold. For the two-bar truss problem this implies that (24) and (26) must be the same (see Appendix B).

Figure 4 shows the displacement sensitivities at $\hat{\mathbf{x}}$ for both formulations for the two-bar truss over the relevant time domain $[t_1, t_1 + T_\omega/2]$, where we assume $t_1 = 200$. The figure shows that the displacement sensitivities of the final ESLM static response sub-problem in $\hat{\mathbf{x}}$ do not coincide with the displacement sensitivities of the dynamic response problem.

Since the displacement sensitivities differ for both formulations, the sensitivities of dynamic compliance objective will also differ at $\hat{\mathbf{x}}$. Figure 5 shows the gradients of the objective in $\hat{\mathbf{x}}$. It can be seen that both vectors differ in direction and magnitude. The values are obtained by evaluating the analytical expressions (see Appendix B) at $\hat{\mathbf{x}}$. The values are listed in Tables 1 and 3. The left figure shows the contour lines of the original dynamic response problem. The right figure shows the contour lines of the objective function in the final ESLM sub-problem based on the equivalent static load evaluated at $\mathbf{x}^k = \hat{\mathbf{x}}$. Figure 4 and Figure 5 both confirm that the KKT conditions for both formulations are not identical, thus, a primal dual KKT point to the ESLM is not in general a primal dual KKT point of the dynamic response problem.

Table 3: Value of dynamic compliance function and its sensitivities evaluated at $\hat{\mathbf{x}}$ obtained from the analytical solution.

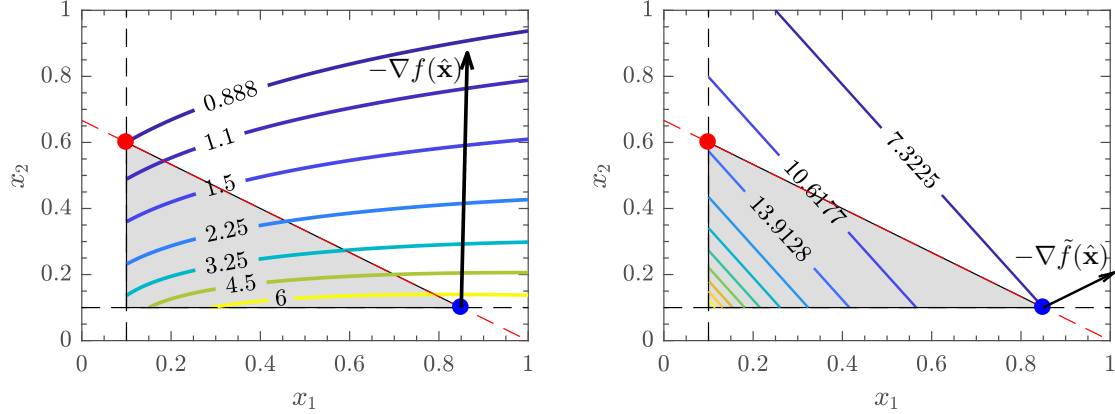| $f_c(\hat{\mathbf{x}})$	$\dfrac{\partial f_c(\hat{\mathbf{x}})}{\partial x_1}$	$\dfrac{\partial f_c(\hat{\mathbf{x}})}{\partial x_2}$
7.32253	-0.67953	-38.58370

16

Figure 5: Contour lines of the objective function values for the dynamic response problem (P_C^{II}) (left) and the final static response problem (S_C^{II}) (right).

5.3.2 Approach 2: The KKT conditions of the dynamic response problem evaluated at $(\hat{\mathbf{x}}, \hat{\boldsymbol{\lambda}})$ are not satisfied

Alternatively, we evaluate the first-order optimality conditions of problems (P_C^{II}) and (P_D^{II}) at the point $(\hat{\mathbf{x}}, \hat{\boldsymbol{\lambda}})$. The KKT conditions of the dynamic response problem evaluated at $(\hat{\mathbf{x}}, \hat{\boldsymbol{\lambda}})$ are

$$\nabla \mathcal{L}(\hat{\mathbf{x}}, \hat{\boldsymbol{\lambda}}) = \nabla f_c(\hat{\mathbf{x}}) + \hat{\lambda} \nabla v(\hat{\mathbf{x}}) - \hat{\boldsymbol{\xi}} + \hat{\boldsymbol{\mu}} = \mathbf{0}, \tag{18a}$$

$$v(\hat{\mathbf{x}}) \leq 0, \quad \hat{\lambda} \geq 0, \tag{18b}$$

$$\underline{\mathbf{x}} - \hat{\mathbf{x}} \leq \mathbf{0}, \quad \hat{\boldsymbol{\xi}} \geq \mathbf{0}, \tag{18c}$$

$$\hat{\mathbf{x}} - \overline{\mathbf{x}} \leq \mathbf{0}, \quad \hat{\boldsymbol{\mu}} \geq \mathbf{0}, \tag{18d}$$

$$v(\hat{\mathbf{x}})\hat{\lambda} = 0, \tag{18e}$$

$$(\underline{x} - \hat{x}_i)\hat{\xi}_i = 0, \quad i = 1, 2, \tag{18f}$$

$$(\hat{x}_i - \overline{x}_i)\hat{\mu}_i = 0, \quad i = 1, 2. \tag{18g}$$

For this particular problem, the constraints in both the static response sub-problem (S_C^{II}) and the dynamic response problem (P_C^{II}) are identical. Thus, the complementarity and the primal and dual feasibility conditions of the dynamic problem are satisfied. However, we will demonstrate that the stationarity condition (18a) is not satisfied.

Remark 6. *Note that the same conclusion can be drawn for the discrete time domain optimization problem (P_D^{II}).*

For the given Lagrange multipliers $\hat{\boldsymbol{\lambda}}$ associated with primal solution $\hat{\mathbf{x}}$ of the ESLM (see (17), the optimality condition (18a) is not satisfied since

$$\nabla \mathcal{L}(\hat{\mathbf{x}}, \hat{\boldsymbol{\lambda}}) = \begin{pmatrix} 7.30868 \\ -33.25823 \end{pmatrix} \neq \mathbf{0}.$$

This result confirms that the primal dual KKT point $(\hat{\mathbf{x}}, \hat{\boldsymbol{\lambda}})$ does not satisfy the KKT conditions of the dynamic response problem, and thus it is not an optimal design.

17

5.4 The point $\hat{\mathbf{x}}$ is not a KKT point of the dynamic response problems $(\mathbf{P}_{\mathbf{C}}^{\mathbf{II}})$ and $(\mathbf{P}_{\mathbf{D}}^{\mathbf{II}})$

We have previously shown that the primal dual KKT point $(\hat{\mathbf{x}}, \hat{\boldsymbol{\lambda}})$ resulting from the ESLM is not in general a KKT point of the dynamic response problem. Additionally, in this particular case, there are no non-negative Lagrange multipliers $\tilde{\boldsymbol{\lambda}}$ associated to the primal point $\hat{\mathbf{x}}$ that satisfy the KKT conditions.

The values for the Lagrange multipliers for the dynamic response problem can be explicitly defined in terms of the sensitivities of the response functions. Substituting the values of the sensitivities of the objective function listed in Table 3 gives

$$
\begin{aligned}
\tilde{\lambda} &= -\frac{\partial f_c(\hat{\mathbf{x}})}{\partial x_1} \left(\frac{\partial v(\hat{\mathbf{x}})}{\partial x_1} \right)^{-1} = 0.67953 \\
\tilde{\xi}_2 &= \frac{\partial f_c(\hat{\mathbf{x}})}{\partial x_2} + \hat{\lambda} \frac{\partial v(\hat{\mathbf{x}})}{\partial x_2} = -37.56441.
\end{aligned}
\tag{19}
$$

The latter part of (19) violates the (dual) feasibility condition (18c). Therefore, the point $\hat{\mathbf{x}}$ is not a KKT point and consequently it is not a local minimum.

5.5 The point $\mathbf{x}^*$ is a KKT point of the dynamic optimization problems $(\mathbf{P}_{\mathbf{C}}^{\mathbf{II}})$ and $(\mathbf{P}_{\mathbf{D}}^{\mathbf{II}})$

Figure 2 suggests that $\mathbf{x}^*$ is a local minimum of the dynamic response problem for the two-bar truss example. At $\mathbf{x}^*$, the volume constraint and the lower bound of x_1 are the active constraints, and therefore, $\xi_2^* = \mu_1^* = \mu_2^* = 0$ to fulfill the complementarity conditions. The Lagrange multipliers associated with the active constraints that satisfy the optimality condition, can be written explicitly in terms of the response sensitivities (see Table 4) as

$$
\begin{aligned}
\lambda^* &= -\frac{\partial f_c(\mathbf{x}^*)}{\partial x_2} \left(\frac{\partial v(\mathbf{x}^*)}{\partial x_2} \right)^{-1} = 1.03755 \\
\xi_1^* &= \frac{\partial f_c(\mathbf{x}^*)}{\partial x_1} + \lambda^* \frac{\partial v(\mathbf{x}^*)}{\partial x_1} = 2.27280
\end{aligned}
\tag{20}
$$

Table 4: Value of dynamic compliance function and its sensitivities evaluated at $\mathbf{x}^*$ obtained from the analytical solution.

$f_c(\mathbf{x}^*)$	$\dfrac{\partial f_c(\mathbf{x}^*)}{\partial x_1}$	$\dfrac{\partial f_c(\mathbf{x}^*)}{\partial x_2}$
0.88811	1.23525	-1.55632

These Lagrange multipliers satisfy the (dual) feasibility conditions. Consequently, the point $(\mathbf{x}^*, \boldsymbol{\lambda}^*)$ *is* a KKT point to the dynamic problem.

The numerical experiments confirm that the SQP method applied to the dynamic response optimization problem $(\mathbf{P}_{\mathbf{D}}^{\mathbf{II}})$ converges to this point. Table 5 contains the objective function value and its sensitivities evaluated at $\mathbf{x}^*$ using two different numerical integration schemes. Additionally, the table contains the Lagrange multipliers values λ^* and ξ_1^* and the number of iterations required for `fmincon` to converge.

Table 5: Value of the dynamic compliance function from $(\mathcal{G}_D)$ and its sensitivities evaluated at $\mathbf{x}^*$ using two different numerical integration approaches, Lagrange multipliers of the active constraints, and the number of iterations that the solver needs to converge to $(\mathbf{x}^*, \boldsymbol{\lambda}^*)$.

Method	$f(\mathbf{x}^*)$	$\dfrac{\partial f(\mathbf{x}^*)}{\partial x_1}$	$\dfrac{\partial f(\mathbf{x}^*)}{\partial x_2}$	λ^*	ξ_1^*	SQP itn.
SQP+Newmark's	0.88764	1.23426	-1.55548	1.03699	2.27125	3
SQP+Runge Kutta	0.88811	1.23525	-1.55632	1.03755	2.27280	2

6 Why does the ESLM show this behaviour?

The engineering explanation to the ESLM behaviour is related to the different properties of the structures which are sought by the static response problems and the dynamic response problems, respectively. For the two-bar truss examples the static response sub-problems attempt to make the structure as stiff as possible with respect to the equivalent static loads without any consideration to the way in which this affects the eigenfrequency of the structure. The dynamic response problem, on the other hand, favors designs which moves the system eigenfrequency away from the driving frequency with much less focus on the static stiffness of the structure. These two type of problems thus suggest designs with different properties, which gives an engineering explanation for the failure of ESLM when applied to these examples.

The explanation from an optimization perspective is a combination of two closely related issues. Firstly, the ESLM algorithm has no mechanism to promote convergence to a KKT point of the original dynamic response problem. Numerical optimization methods such as SQP would normally employ one of the several available approaches such as a merit function combined with a back-tracking line-search or a trust-region approach, see e.g. [11]. Secondly, the quality of the approximation from the ESLM sub-problem is not sufficiently good to ensure standard descent properties. These issues can be (partly) illustrated by again studying the two-bar truss problem. For the purpose of presentation we here assume that the volume constraint is stated as an equality constraint. This implies that the feasible set simplifies to the set $\{\mathbf{x} \in \mathbb{R}^2 \mid \mathbf{x} = (1 - \beta)\mathbf{x}^* + \beta\hat{\mathbf{x}} \text{ for } \beta \in [0, 1]\}$. Since problem $(\mathcal{S}_C)$ is a linearly constrained nonlinear problem a suitable merit function is the objective function itself. Here we assume that the iterates are all feasible. A commonly used idea in numerical optimization is to ensure descent in the merit function, i.e. to require that $f(\mathbf{x}^k + \alpha\mathbf{d}^k) < f(\mathbf{x}^k)$ where $\alpha > 0$ is the step length and $\mathbf{d}^k$ is a (feasible) search direction. To ensure convergence in line-search methods is often requested that the step-length is such that a condition ensuring sufficient decrease is satisfied. One such condition is the Armijo condition ([11])

$$f(\mathbf{x}^k + \alpha\mathbf{d}^k) \leq f(\mathbf{x}^k) + \mu\alpha\nabla f(\mathbf{x}^k)^T\mathbf{d}^k$$

where $\mu > 0$ is a given parameter. In the ESLM we can interpret $\mathbf{d}^k = \mathbf{x}^k - \hat{\mathbf{x}}^k$ as a candidate search direction. The issue is that, despite the convexity of the sub-problem $(\mathrm{S}_{\mathrm{C}}^{\mathrm{II}})$ the direction is not generally a descent direction for the objective function of the dynamic response problem $(\mathrm{P}_{\mathrm{C}}^{\mathrm{II}})$ which would result in failure of the line-search, i.e. the step-length becomes zero. In the ESLM no such test is done and the objective function value of the dynamic response problem is allowed to increase between two updates of the iterates in Algorithm 1. This is illustrated in Figure 6 where the objective function of
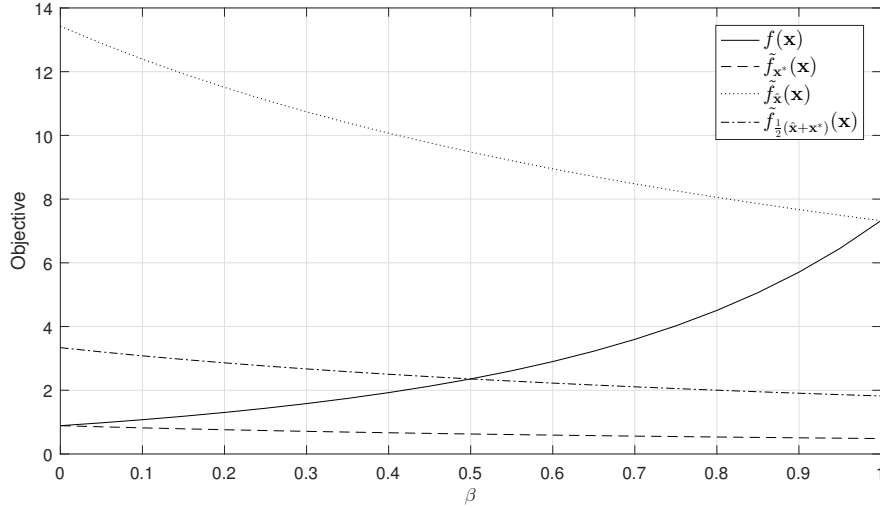
Figure 6: Objective function of the dynamic response problem ($\mathrm{P_D^{II}}$) and two ESLM static response sub-problems for all designs satisfying the volume constraint with equality, i.e. for $\mathbf{x}(\beta) = (1 - \beta)\mathbf{x}^* + \beta\hat{\mathbf{x}}$ with $\beta \in [0, 1]$.

the dynamic response problem is plotted together with the objective function of the ESLM static response sub-problem with equivalent static loads evaluated at the three designs $\mathbf{x}^*$, $(1/2)(\mathbf{x}^* + \hat{\mathbf{x}})$, and $\hat{\mathbf{x}}$. The plots are done for all designs satisfying the volume constraint with equality. The figure shows that the static response sub-problem objective correctly estimates the objective function value of the dynamic response objective at the point but does not correctly capture the design sensitivities. The figure also illustrates that the sub-problem objective function can either underestimate (dashed line) or overestimate (dotted line) the dynamic response objective over the entire feasible set. It can also be inconsistent in this respect as illustrated by the dash-dotted line. This implies that the overall quantitative properties of the approximation change from iterate to iterate. Another observation from Figure 6 is that the static response sub-problem very inaccurately approximates the dynamic response problem, even short distances away from the point in which the ESLs are computed. The figure also shows that for this case the ESLM does in fact converge to a local optimum (and a KKT point). *The ESLM converges to a local and global maximizer of the dynamic response problem (P_C^{II}).*

6.1 Quality of the ESLM approximation

In the two-bar truss example, the driving frequency was originally chosen as $\omega = \pi/2$, which was in the same order as the values of the natural frequency for the different two-bar truss configurations in the feasible set. Next, we study the effect of lowering the driving frequency, while keeping all other problem parameters the same. Notice that the optimal ESLM design for this two-bar truss problem is independent of the equivalent static load, and therefore, the optimal ESLM design is $\hat{\mathbf{x}} = (0.85\ 0.1)^T$ irrespective of the driving frequency.

Figure 7 compares the objective function of the final sub-problem in the ESLM at $\hat{\mathbf{x}}$ with the objective function of the dynamic response problem for decreasing driving frequencies $\pi/32$ and $\pi/64$. It can be seen that, lowering the driving frequency with respect to the

20

natural frequency, leads to the ESLM approximating better the original dynamic response problem.

The increasingly improved approximation for lower driving frequencies is confirmed for this particular problem by plotting the displacement sensitivities for both formulations in Figure 8. It can be seen that the displacement sensitivities of the ESLM approximate the displacement sensitivities better than in the original problem in Figure 4.

We conclude that the more quasi-static the behaviour of the original dynamic response problem, the better the approximation of the ESLM. However, when the problem is quasi-static one could argue that there is no need for the ESLM since solving the quasi-static problem is less computationally expensive.

7   Discussions

Although the two-bar truss examples are both small-scale and not representative of industrial structural optimization problems they satisfy the most important properties that can be expected in dynamic response structural optimization in terms of the structural analysis and sensitivity analysis models and techniques. The problem is a sizing problem and the issues arising from topology optimization, such as vanishing of members and constraints, are not present and can thus not be responsible for the behavior the algorithm displays. The ESLM also shows similar behaviour using different time integration techniques and using analytical solutions to the governing equations. The time discretization is thus not responsible for the displayed behaviour. The examples are therefore sufficient to illustrate that the ESLM cannot in general be ensured to provide KKT points and to motivate the title of the article.

The examples illustrate several important points regarding the theoretical convergence properties of the ESLM. The sequence of iterations obtained from the ESLM for the two-bar truss is almost independent of the starting point. In particular, if the ESLM (for the two-bar truss problem) is started at a KKT point of the original dynamic response problem then the ESLM moves away and does not return. *This illustrates that the ESLM does not in general guarantee descent in the objective function.*

The stopping criterion used for the ESLM is based on the norm of the difference between two consecutive iterates. This stopping criterion is stronger than the criterion suggested in e.g. [12] which is based on the difference of two consecutive equivalent static loads. The examples thus illustrate that it is not possible to assure better theoretical convergence properties by this change of stopping criterion.

The static response sub-problems for the various versions of the example have excellent theoretical properties from an optimization point of view. They are (equivalent to) convex problems, they satisfy standard constraint qualifications, and each enjoys a unique optimal solution. This is, from a numerical optimization perspective, a best case scenario. Most academical and industrial applications will (likely) not satisfy most, or any, of these properties. One can thus argue that the ESLM will likely not behave as a good optimization method for more advanced and larger problems. On the other hand, the examples are very small-scale, have been purposely designed to show poor behaviour of the algorithm, and one can thus argue that the ESLM generally does not behave as poorly as illustrated by these examples. This discussion thus suggests that the ESLM must be numerically benchmarked against classical gradient based numerical optimization methods such as SQP or interior-point methods on a large set of well-documented and publicly available benchmark problems.
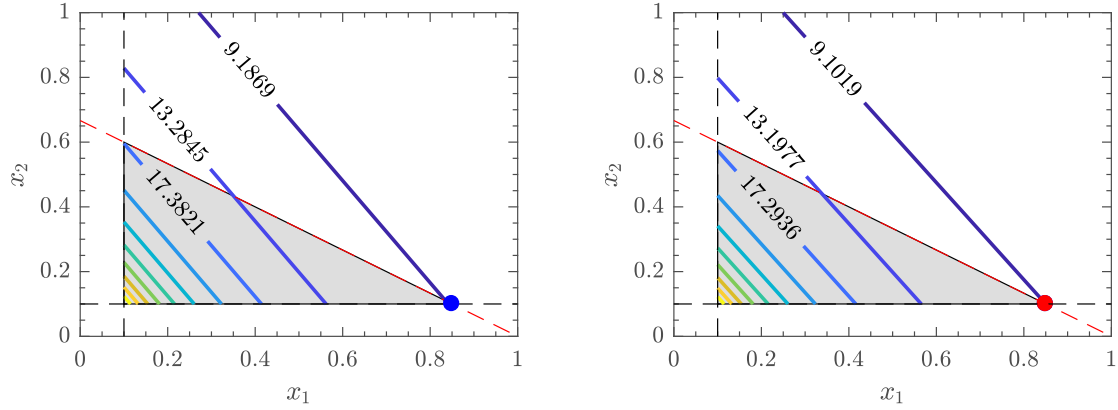
(a) $\omega = \pi/32$
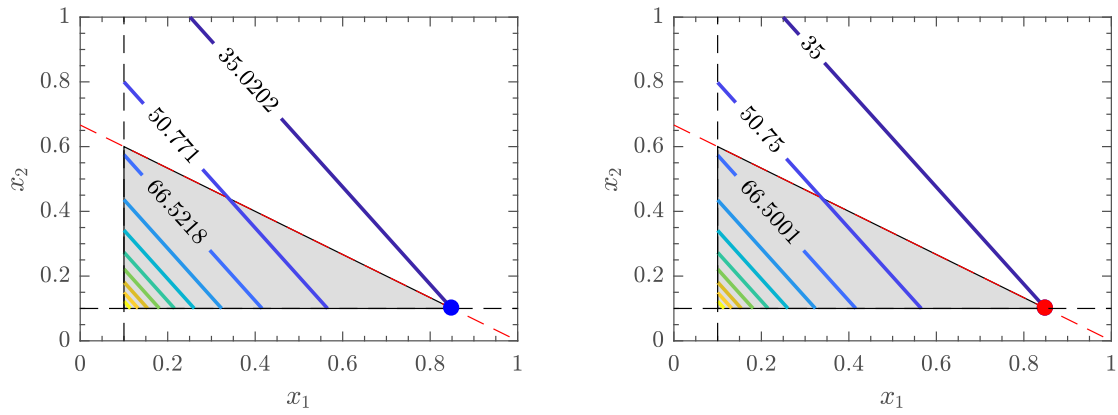
(b) $\omega = \pi/64$

Figure 7: Effect of lowering the driving frequency ω. Objective function for the ESLM final static response sub-problem (S_C^{II}) at $\hat{\mathbf{x}}$ (left), and the dynamic response optimization problem (P_C^{II}) (right).
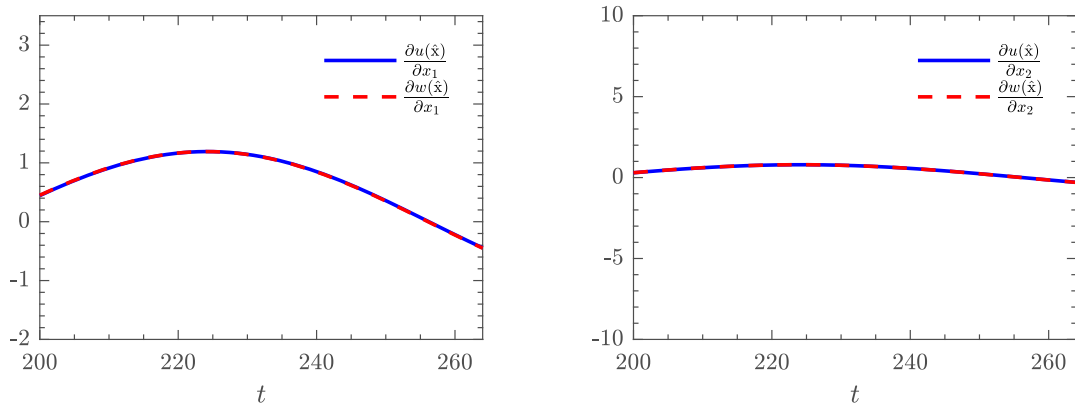

Figure 8: Displacement sensitivities at the point $\hat{\mathbf{x}}$ for both problem formulations and a lower driving frequency of $\omega = \pi/64$. Displacement sensitivities with respect to x_1 (left), and displacement sensitivities with respect to x_2 (right).

22

8   Conclusions

The presented counter examples show that the Equivalent Static Loads Method as currently developed cannot theoretically ensure to find a KKT point, and therefore, optimal design to the considered dynamic response structural optimization problem. This conclusion remains valid even in the situation that strengthened stopping criteria are satisfied.

Acknowledgements

References

[1] W. Achtziger, M. Bendsøe, A. Ben-Tal, and J. Zowe. Equivalent displacement based formulations for maximum strength truss topology design. *Impact of Computing in Science and Engineering*, 4(4):315–345, 1992.

[2] M.P. Bendsøe and O. Sigmund. *Topology Optimization — Theory, Methods and Applications*. Springer, 2003.

[3] S. Boyd and L. Vandenberghe. *Convex optimization*. Cambridge University Press, 2004.

[4] K.K. Choi and N.-H. Kim. *Structural Sensitivity Analysis and Optimization 1*. Springer, 2005.

[5] W.S. Choi and G.J. Park. Transformation of dynamic loads into equivalent static loads based on modal analysis. *International Journal for Numerical Methods in Engineering*, 46(1):29 – 43, 1999.

[6] W.S. Choi and G.J. Park. Structural optimization using equivalent static loads at all time intervals. *Computer Methods in Applied Mechanics and Engineering*, 191:2077 – 2094, 2002.

[7] R.D. Cook, D.S. Malkus, and M.E. Plesha. *Concepts and applications of finite element analysis*. Wiley, 2002.

[8] B.S. Kang, W.S. Choi, and G.J. Park. Structural optimization under equivalent static loads transformed from dynamic loads based on displacement. *Computers & Structures*, 79(2):145 – 154, 2001.

[9] D.G. Luenberger and Y. Ye. *Linear and Nonlinear Programming*. Springer, 4th edition, 2016.

[10] G.L. Nemhauser and L.A Wolsey. *Integer and Combinatorial Optimization*. John Wiley and Sons, 1999.

[11] J. Nocedal and S.J. Wright. *Numerical Optimization*. Springer, New York, 2006.

[12] G.J. Park and B.S. Kang. Validation of a structural optimization algorithm transforming dynamic loads into equivalent static loads. *Journal of Optimization Theory and Applications*, 118(1):191 – 200, 2003.

[13] L.F. Shampine and M.W. Reichelt. The MATLAB ODE suite. *SIAM Journal on Scientific Computing*, 18(1):1–22, 1997.

[14] M.K. Shin, K.J. Park, and G.J. Park. Optimization of structures with nonlinear behavior using equivalent loads. *Computer Methods in Applied Mechanics and Engineering*, 196(4-6):1154 – 1167, 2007.

[15] M. Stolpe. On the equivalent static loads approach for dynamic response structural optimization. *Structural and Multidisciplinary Optimization*, 50(6):921–926, 2014.

[16] K. Svanberg. On the convexity and concavity of compliances. *Structural optimization*, 7(1):42–46, 1994.

Appendix A A worst-case two-bar truss example

An alternative time-discretized version of the truss example is the worst-case version of problem $(\mathcal{P}_D)$ which reads

$$
\begin{aligned}
&\underset{\mathbf{x}\in\mathbb{R}^n}{\text{minimize}} \quad \max_{\ell_1\leq i\leq \ell_2}\{\Delta t\mathbf{u}_i(\mathbf{x})^T\mathbf{K}(\mathbf{x})\mathbf{u}_i(\mathbf{x})\} \\
&\text{subject to} \quad \mathbf{x}\in X.
\end{aligned}
\tag{21}
$$

Problem (21) is in general non differentiable and is therefore reformulated into

$$
\begin{aligned}
&\underset{\mathbf{x}\in\mathbb{R}^n,\tau\in\mathbb{R}}{\text{minimize}} \quad \tau \\
&\text{subject to} \quad \Delta t\mathbf{u}_i(\mathbf{x})^T\mathbf{K}(\mathbf{x})\mathbf{u}_i(\mathbf{x})\leq \tau \quad i=\ell_1,\ell_1+1,\ldots,\ell_2 \\
&\qquad\qquad \mathbf{x}\in X, \tau\geq 0.
\end{aligned}
\tag{22}
$$

Problem (22) satisfies the format considered in e.g. [12] in that the objective function is independent of the displacements and the nonlinear constraints only consider one time step per constraint. The static response sub-problem to be solved in the ESLM at iteration k corresponding to (22) becomes

$$
\begin{aligned}
&\underset{\mathbf{x}\in\mathbb{R}^n,\tau\in\mathbb{R}}{\text{minimize}} \quad \tau \\
&\text{subject to} \quad \tilde{f}_{i,\mathbf{x}^k}(\mathbf{x})=\Delta t(\mathbf{r}_i^e(\mathbf{x}^k))^T\mathbf{K}^{-1}(\mathbf{x})\mathbf{r}_i^e(\mathbf{x}^k)\leq \tau \quad i=\ell_1,\ell_1+1,\ldots,\ell_2 \\
&\qquad\qquad \mathbf{x}\in X, \tau\geq 0.
\end{aligned}
\tag{23}
$$

Problem (23) enjoys similar properties as the static response sub-problem $(\mathcal{S}_D)$. The objective function is linear and the constraint functions are convex resulting in a convex feasible set. The feasible set of (23) is non-empty since for any $\mathbf{x}\in X$ it is possible to find a sufficiently large $\tau>0$ such that the nonlinear constraints are satisfied. Additionally, the feasible set is convex and it is possible to find a feasible point $(\mathbf{x},\tau)$ with $\mathbf{x}\in \text{int}(X)$ and $\tau>0$, i.e. the Slater constraint qualifications [3] are satisfied for (23). Again, uniqueness of the

optimal solution is not guaranteed in the general case, but is ensured for the two-bar truss example.

For the two-bar truss the static response sub-problem for the worst-case situation becomes

$$\begin{array}{ll}
\underset{\mathbf{x}\in\mathbb{R}^2,\tau\in\mathbb{R}}{\text{minimize}} & \tau \\
\text{subject to} & \frac{\Delta t}{x_1+\frac{2}{3}x_2}(r_i^e(\mathbf{x}^k))^2 \leq \tau \quad \text{for } i = \ell_1, \ell_1+1, \ldots, \ell_2 \\
& \mathbf{x} \in X, \tau \geq 0.
\end{array}$$

Solving the static response sub-problem for the two-bar truss problem can again be done analytically and in the same manner as for the first version of the problem, i.e. the optimal solution is again unique and given by $\hat{\mathbf{x}}$ independent of the equivalent static loads (under the condition that at least one is non zero). The equivalent static loads methods from Algorithm 1 thus converges in the same manner as before, i.e. at most two static response sub-problems are solved.

The point $\mathbf{x}^*$ is also found numerically using the optimization approaches as outlined in Section 5. The point is verified as a KKT point to the dynamic response problem (22) in the following way. At the point $\mathbf{x}^*$ the max in the objective function in (21) is attained in one time step i^* and the directional derivatives $\nabla f_{i^*}(\mathbf{x}^*)^T\mathbf{d}$ in the two feasible directions $\mathbf{d}_1^* = \hat{\mathbf{x}} - \mathbf{x}^* = \frac{1}{4}(3 \ -2)^T$ and $\mathbf{d}_2^* = (0 \ -1)^T$ are both strictly positive. Since these two vectors span the tangent cone at $\mathbf{x}^*$ and constraint qualifications are satisfied the point is as a KKT point. Our numerical experiments also show that the SQP method applied directly to (22) finds Lagrange multipliers such that the KKT conditions for (22) are accurately satisfied.

The point $\hat{\mathbf{x}}$ does however not correspond to a KKT point to the dynamic response problem (22). Evaluating the dynamic response at for the design $\hat{\mathbf{x}}$ shows that the maximum in (21) is attained at one time-point $\hat{i}$. This implies that the objective function in (21) is differentiable at the point $\hat{\mathbf{x}}$. The derivative with respect to the design variables is given by $\nabla f_{\hat{i}}(\hat{\mathbf{x}})$. The directional derivatives $\nabla f_{\hat{i}}(\hat{\mathbf{x}})^T\hat{\mathbf{d}}_1 < 0$ and $\nabla f_{\hat{i}}(\hat{\mathbf{x}})^T\hat{\mathbf{d}}_2 > 0$. This shows that $\hat{\mathbf{x}}$ does not correspond to a KKT point of (22).

Appendix B   Analytical design sensitivities

The design sensitivity of the displacement with respect to the jth design variable becomes

$$\frac{\partial u(\mathbf{x},t)}{\partial x_j} = \frac{\partial u_0}{\partial x_j}\sin(\omega t + \phi(\mathbf{x})) + \frac{u_0(\mathbf{x})}{1+\beta(\mathbf{x})}\frac{\partial \beta(\mathbf{x})}{\partial x_j}\cos(\omega t + \phi(\mathbf{x})), \qquad (24)$$

where

$$\frac{\partial u_0(\mathbf{x})}{\partial x_j} = -\frac{u_0^3(\mathbf{x})}{r_0^2}\left(k(\mathbf{x}) - w^2 m(\mathbf{x})\right)\left(\frac{\partial k(\mathbf{x})}{\partial x_j} - \omega^2 \frac{\partial m(\mathbf{x})}{\partial x_j}\right),$$

and

$$\frac{\partial \beta(\mathbf{x})}{\partial x_j} = \frac{\beta^2(\mathbf{x})\omega_n(\mathbf{x})}{2k(\mathbf{x})\zeta(\mathbf{x})\omega}\left(\frac{\partial k(\mathbf{x})}{\partial x_j} - \omega^2\frac{\partial m(\mathbf{x})}{\partial x_j}\right).$$

The design sensitivity of the dynamic compliance $\dfrac{\partial f_c(\mathbf{x},t)}{\partial x_j}$ can be written as

$$\frac{\partial f_c(\mathbf{x},t)}{\partial x_j} = \left(\frac{2}{u_0(\mathbf{x})}\frac{\partial u_0(\mathbf{x})}{\partial x_j} + \frac{1}{k(\mathbf{x})}\frac{\partial k(\mathbf{x})}{\partial x_j}\right)f_c(\mathbf{x},t), \qquad (25)$$

which is valid for a time domain of duration $T_\omega/2$ for which the compliance is independent of the phase shift.

Inside the kth static response sub-problem, the design sensitivity of the displacement is

$$\frac{\partial w(\mathbf{x}, t)}{\partial x_j} = -\frac{1}{(k(\mathbf{x}))^2} \frac{\partial k(\mathbf{x})}{\partial x_j} r^e(\mathbf{x}^k, t) \tag{26}$$

and the design sensitivity of the the dynamic compliance is

$$\frac{\partial \tilde{f}_{c,\mathbf{x}^k}(\mathbf{x}, w(\mathbf{x}, t))}{\partial x_j} = -\frac{1}{k(\mathbf{x})} \frac{\partial k(\mathbf{x})}{\partial x_j} \tilde{f}_{c,\mathbf{x}^k}(\mathbf{x}, w(\mathbf{x}, t)). \tag{27}$$